A DISSERTATION ON

Synthesis and Characterization of $Na_{0.67}Mn_{0.65}Fe_{0.20}Ni_{0.15}O_2$ as Cathode Material for Sodium Ion Batteries

submitted in partial fulfilment of
the requirement for the degree of

Masters of Technology
In
NanoScience and Technology

By

Nikita Jain

(2K12/NST/10)

Under the Supervision of

Dr. Amrish K. Panwar

Department of Applied Physics

Delhi Technological University

(Formerly Delhi College Of Engineering)

New Delhi-110042

Department of Applied Physics

Delhi Technological University

Delhi

CERTIFICATE

This is to certify that Mrs. Nikita Jain, a student of final semester M.Tech (NanoScience and Technology), Applied Physics Department, during the session 2012-2014 has successfully completed the project work entitled as **"Synthesis and Characterization of $Na_{0.67}Mn_{0.65}Fe_{0.20}Ni_{0.15}O_2$as Cathode Material for Sodium Ion Batteries"** Delhi Technological University, Delhi and has submitted a satisfactory report in partial fulfilment for the award of the degree of Master of Technology.

The assistance and help received during the course of investigation have been fully acknowledged.

Date: 31-07-2014

Dr.Amrish K. Panwar Signature ……. Date ……
(Supervisor)

Prof. S.C. Sharma Signature ……. Date ……
(Head of the Department)

CANDIDATE'S DECLARATION

I hereby declare that the work which is being presented in this thesis entitled **"Synthesis and Characterization $Na_{0.67}Mn_{0.65}Fe_{0.20}Ni_{0.15}O_2$ as Cathode Material for Sodium-Ion Batteries"** is my own work carried out under the supervision of Dr. Amrish. K. Panwar, Assistant Professor, Delhi Technological University, Delhi.

I further declare that the matter embodied in this thesis has not been submitted for the award of any other degree or diploma.

Date: Nikita Jain

Place: New Delhi Roll No. - 2K12 /NST/10

ACKNOWLEDGEMENTS

With great pleasure I would like to express my first and sincere gratitude to my Supervisor **Dr. AMRISH K. PANWAR**(Assistant Professor, Department of Applied Physics, DTU)for his continuous support, patience, motivating ideas , enthusiasm and immense knowledge. His guidance always enlightens and helped me to shape my work.

Besides my Supervisor , I would like to express my deep gratitude and respect to Dr. **S.C. Sharma** , Prof. and Head of Department of Physics, DTU, for his encouragement , insightful comments and valuable suggestions during the course.

I humbly extend my words of gratitude to other faculty members, staff and administration of this department for providing me the valuable support and time whenever required. Thanks to all of them for questioning me about my ideas, helping me think rationally and even for hearing my problems.

I am deeply grateful to the research scholars namely; Mr. Rakesh Saroha, Mr. Aditya Jain, Ms Lucky Krishna, Mrs. Ritu for helping me to perform this work.

I would also like to thanks my supportive friends and others who made specially, the labs a friendly environment for working.

LIST OF FIGURES

LIST OF ABBREVIATIONS

NIBs: Sodium-ion batteries

LIBs: Lithium-ion batteries

Li: Lithium

Na: Sodium

NaMFN: $Na_{0.67}Mn_{0.65}Fe_{0.20}Ni_{0.15}O_2$

XRD: X-Ray Diffraction

SEM: Scanning-Electron Microscope

Na_f : Sodium which shares the face with MO_6octahedra

Na_e: Sodium which shares the edge with MO_6octahedra

nm: Nanometer

ABSTRACT

The major contribution to the battery performance is due to the cathode material. Stable sodium ion storage cathodes with adequate reversible capacity are now greatly needed for enabling Sodium-ion battery technology for large scale and low cost electric storage applications.

The deintercalation and intercalation of sodium in various layered Na_xMO_2 has been reported for a very wide variety of transition metals as briefly outlined in a recent report[5]. The manganese and cobalt oxides are the most viable for positive electrodes. But cobalt is toxic and expensive. The Jahn-Teller distortion of Mn(III) is the most prominent factor which decides the structural stability for Mn-based oxides during ion insertion. Hence a general strategy applied to sodium based layered oxides is to substitute partial metal ions in the transition metal layer using selective cations, to improve the structural stability and electrochemical performances of the layered cathode host.

In light of the better Lithium-ion storage performance of layered oxides, sodium based $Na_{0.67}Mn_{0.65}Fe_{0.20}Ni_{0.15}O_{2,}$ cathode material was synthesized by sol-gel method using citric acid as chelating agent. Synthesized $Na_{0.67}Mn_{0.65}Fe_{0.20}Ni_{0.15}O_2$ has been characterized by X-ray diffractometer (XRD) to confirm the proper phase formation. Scanning Electron Microscope (SEM) for structural and morphological studies. The XRD measurement demonstrated that the sample have a pure P2 phase.

TABLE OF CONTENTS

CHAPTER 1: INTRODUCTION

Owing to the almost unmatched volumetric energy density and high cell voltage, lithium ion batteries(LIBs) have dominated the portable electronic industry for the last twenty years[1]. Beyond consumer electronics, LIBs are also growing in popularity for military, electric vehicle and aerospace applications. But due to the high cost, hazardness and delicacy of lithium, one need to replace an alternative energy storage material.

The pressing needs for better energy storage technologies in large-scale applications that are economically feasible, particularly for the deployment of renewable energy sources, are strong drivers for fundamental research in new materials discovery and their electrochemistry. Li-ion batteries offer the highest energy density among all secondary battery technologies, have dominated the portable electronics market and have been chosen to power the next generation of electric vehicles and plug-in electric vehicles[2]. Nevertheless, the concerns regarding the size of the lithium reserves and the cost associated with Li-ion technology have driven the researchers to search more sustainable alternative energy storage solutions. In this light, sodium-based intercalation compounds have made a major comeback because of the natural abundance of sodium. It is important to point out that sodium based systems would have lower energy density in comparison to lithium based systems because of its intrinsic lower operation voltages. Typical energy densities range from 300-700 Wh/kg as shown in Figure 1[22] given below.

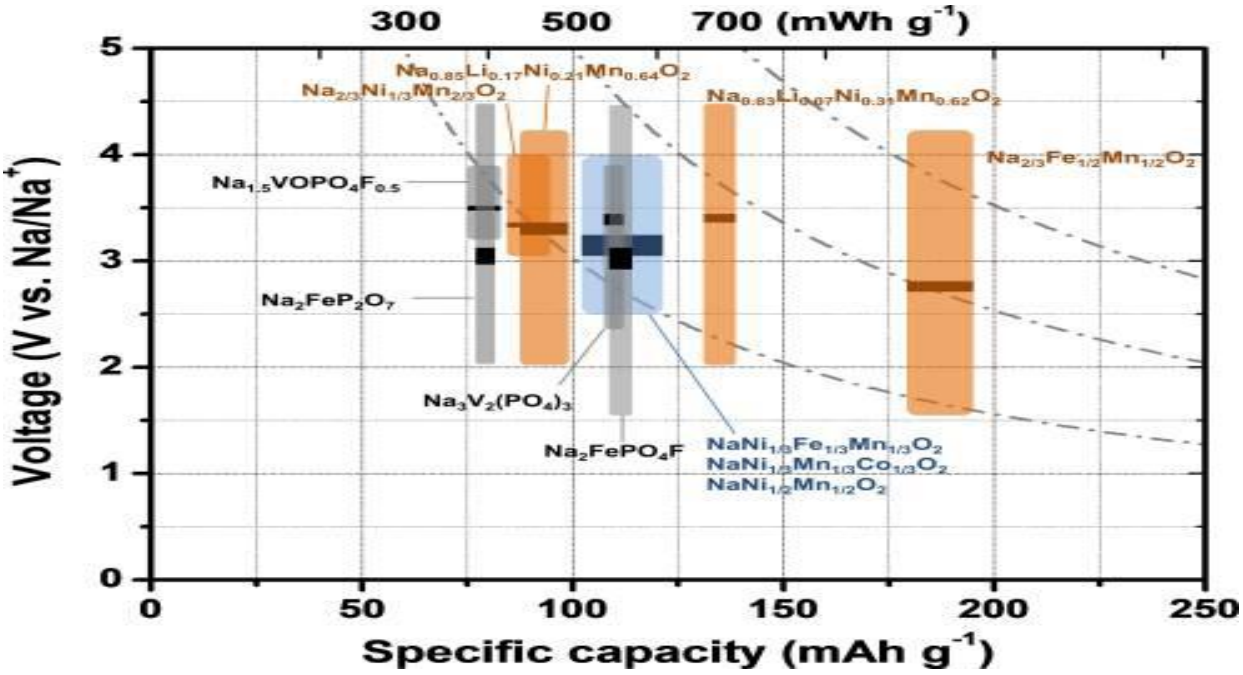

FIGURE 1: ENERGY DENSITIES OF VARIOUS CATHODE MATERIALS FOR SODIUM ION BATTERY

On the other hand, the lower voltages would result in better safety and the possibility of using cheaper water based electrolytes. A more encouraging fact is that the Na-ion diffusion barriers in solid state compounds are comparable to the Li counterparts, indicating that Na-ion systems can be competitive with Li-ion systems in terms of discharge/charge rates. However, the ionic radii of Na-ion is considerably larger than that of Li-ion, more open structures can be made to accommodate large Na-ions and allow fast solid state Na-ion diffusion at room temperature.

The sodium-ion battery field presents many solid state materials design challenges, and rising to that call in the past couple of years, several reports of new sodium-ion technologies and electrode materials have surfaced. These range from high-temperature air electrodes to new layered oxides, polyanion-base materials, carbons and other insertion materials for sodium-ion batteries, many of which hold promise for future sodium-based energy storage applications.

1.1 HISTORY OF BATTERY

A battery is a device consisting of one or more electrochemical cells that convert stored chemical energy into electrical energy. Since the invention of the first battery (or "voltaic pile") in 1800 by Alessandro Volta and then technically improved Daniell cell in 1836, batteries have

become a common power source for various applications such as household and industrial. In the year 2005, the worldwide battery industry generates US$48 billion in sales each year, with 6% annual growth.

In general there are two types of batteries: primary batteries (disposable batteries), which are designed to be used once and discarded, and secondary batteries (rechargeable batteries), which are designed to be recharged and used multiple times. Batteries come in many sizes, from miniature cells used to power hearing aids and wristwatches to battery banks the size of rooms that provide standby power for telephone exchanges and computer data centers.

1.2 TIMELINE OF BATTERIES

In 1798: Italian physicist Alessandro Volta makes the first battery. It was named as "voltaic pile which consists of stacks of zinc, acid-moistened cardboard and copper.

In 1836: English chemist John F. Daniell improves Volta's battery: preventing the corrosion that normally occurs with Volta's batteries. Gaston Plante invented the lead-acid battery in 1859.

In 1868: French chemist Georges Leclanche created the first "wet cell" battery.

In 1888: German scientist Dr. Carl Gassner invented the "dry cell." His battery is similar to the carbon-zinc batteries of today.

In 1896: American dry cell manufacturer, Columbia makes the first commercially available battery. This company turns into Eveready Battery Company- today known as Energizer Battery Company.

In 1898: Conrad Hubert creates the first flashlight; he calls it an, "electric hand torch."

In 1900s: Thomas Alva Edison improves the car battery. His other battery improvements make their way into trains, and mines. This becomes one of Edison's biggest cash generators: meeting or exceeding the light bulb and the motion picture machine.

In 1956: Eveready Battery Company develops the 9-volt battery.

In 1959: Eveready Battery Company develops a commercially available alkaline battery.

In 1960: Miniature silver-oxide batteries or "button batteries" are developed for hearing aides and watches. The first nickel-cadmium rechargeable battery system is developed by WaldmarJunger in Sweden.

In 1992: The first lithium batteries are commercially available. These are the most powerful AA-size batteries on the market.

2000-present: Innovations in rechargeable technology introduce products such as Nickel-Metal hydride rechargeable batteries, titanium high-performance batteries, and 15-minute rechargeable batteries.

Future: The future is both bright and challenging for sodium-ion batteries.

1.3 SODIUM

Sodium is a chemical element with the symbol Na (from Latin: natrium) and atomic number eleven. It is a soft, silvery-white, highly reactive metal and is a member of the alkali metals; its only stable isotope is ^{23}Na. The free metal does not occur in nature, but instead must be prepared from its compounds; it was first isolated by Humphry Davy in 1807 by the electrolysis of sodium hydroxide. Sodium is the sixth most abundant element in the Earth's crust, and exists in numerous minerals such as feldspars, sodalite and rock salt. Many salts of sodium are highly water-soluble, and their sodium has been leached by the action of water so that chloride and sodium are the most common dissolved elements by weight in the Earth's bodies of oceanic water.

Many sodium compounds are useful, such as sodium hydroxide (lye) for soap making, and sodium chloride for use as a deicing agent and a nutrient (edible salt). Sodium is an essential element for all animals and some plants. In animals, sodium ions are used against potassium ions to build up charges on cell membranes, allowing transmission of nerve

impulses when the charge is dissipated. The consequent need of animals for sodium causes it to be classified as a dietary inorganic macro-mineral.

FIGURE 2: THE PERIODIC TABLE

1.5.1 WHY SODIUM ION BATTERY?

DISADVANTAGES OF LITHIUM ION BATTERIES[3]

It is expensive, almost 40% more than nickel cadmium. It is delicate, the battery temperature must be monitored from within (which raises the price), and sealed particularly well. The regulations, when shipping Li-Ion batteries in bulk (which also raises the price). Also it is Class 9 miscellaneous hazardous material.

Drop-In-solution:

Na-ion materials can be processed in the same way as Li-ion materials at every step, from the synthesis of the active materials to the electrode processing. This will allow current Li-ion battery manufacturers to use existing equipment to construct batteries. Existing Li-ion manufacturing lines can be used to make Na-ion batteries. The electrode materials in Li-ion batteries provide the best library for research of Na-ion batteries because many Na-ion insertion hosts have their roots in Li-ion insertion hosts. “In terms of weight and size, batteries have become one of the limiting factors in the development of electronic devices.”

SOME POINTS WHICH MAKES US THINK ABOUT SWITCHING FROM LITHIUM TO SODIUM [4]: The high reduction potential of -2.71V which is just 0.3V above the lithium, low weight, non-toxic nature, relative abundance i.e. sixth most abundant metal(Na ~ 2.6 % vs. Li ~0.005 %) and low cost favors switching from lithium to sodium.

1.5.2 DISADVANTAGES OF SODIUM ION BATTERIES[5]

Ionic volume of sodium is almost twice than that of lithium. Also the molecular weight of sodium is triple. Hence it is difficult to find an insertion host that can readily accept the insertion and extraction of the relatively large sodium ion into its structure.

1.6 SOME TERMS

1. **ENERGY DENSITY**: It is the amount of energy stored in a given system or region of space per unit volume. The energy density is generally expressed in Wh/L. The higher the energy density of the fuel, the more energy may be stored or transported for the same amount of volume. The energy density of a fuel per unit mass is called the specific energy of that fuel.

2. **MEMORY EFFECT**: It describes one very specific situation in which certain batteries gradually lose their maximum energy capacity if they are repeatedly recharged after being only partially discharged. Memory effect, also known as battery effect, lazy battery effect or battery memory, is an effect observed in nickel cadmium rechargeable batteries that causes them to hold less charge. It describes one very specific situation in which certain NiCd batteries gradually lose their maximum energy capacity if they are repeatedly recharged after being only partially discharged. The battery appears to "remember" the smaller capacity. The source of the effect is changes in the characteristics of the underused active materials of the cell. The term is commonly misapplied to almost any case in which a battery appears to hold less charge than was expected. These cases are more likely due to battery age and use, leading to

irreversible changes in the cells due to internal short-circuits, loss of electrolyte, or reversal of cells.

3. **CAPACITY**: A battery's capacity is the amount of electric charge it can store. Unit is mAh/g. The more electrolyte and electrode material there is in the cell the greater the capacity of the cell. A small cell has less capacity than a larger cell with the same chemistry, and they develop the same open-circuit voltage. Because of the chemical reactions within the cells, the capacity of a battery depends on the discharge conditions such as the magnitude of the current (which may vary with time), the allowable terminal voltage of the battery, temperature, and other factors. The available capacity of a battery depends upon the rate at which it is discharged. If a battery is discharged at a relatively high rate, the available capacity will be lower than expected.

   The capacity printed on a battery is usually the product of 20 hours multiplied by the constant current that a new battery can supply for 20 hours at 68 F° (20 C°), down to a specified terminal voltage per cell. A battery rated at 100 Ah will deliver 5 A over a 20-hour period at room temperature. However, if discharged at 50 A, it will have a lower capacity. The relationship between current, discharge time, and capacity for a lead acid battery is approximated (over a certain range of current values) byPeukert's law:

$$t = \frac{Q_P}{I^k}$$

where

Q_P is the capacity when discharged at a rate of 1 amp.

I is the current drawn from battery (A).

t is the amount of time (in hours) that a battery can sustain.

k is a constant around 1.3.

For low values of *I* internal self-discharge must be included.

Internal energy losses and limited rate of diffusion of ions through the electrolyte cause the efficiency of a real battery to vary at different discharge rates. When discharging at low rate, the battery's energy is delivered more efficiently than at higher discharge rates, but if the rate is very low, it will partly self-discharge during the long time of operation, again lowering its efficiency.

Installing batteries with different A·h ratings will not affect the operation of a device (except for the time it will work for) rated for a specific voltage unless the load limits of the battery are exceeded. High-drain loads such as digital cameras can result in delivery of less total energy, as happens with alkaline batteries. For example, a battery rated at 2000 mAh for a 10- or 20-hour discharge would not sustain a current of 1 A for a full two hours as its stated capacity implies.

4. **C RATES**: The C-rate signifies a discharge rate relative to the capacity of a battery in one hour. A rate of 1C would mean an entire 1.6Ah battery would be discharged in 1 hour at a discharge current of 1.6A. A 2C rate would mean a discharge current of 3.2A.

5. **CYCLE LIFE**: It is defined as the number of complete charge - discharge cycles a battery can perform before its nominal capacity falls below 80% of its initial rated capacity.

1.6 OBJECTIVE

- To synthesize $Na_{0.67}Mn_{0.65}Fe_{0.2}Ni_{0.15}O_2$ by sol-gel method with citric acid as chelating agent.
- Characterization of $Na_{0.67}Mn_{0.65}Fe_{0.2}Ni_{0.15}O_2$ using X-Ray Diffractometer Analysis (XRD) and Scanning Electron Microscopy(SEM).

CHAPTER 2: LITERATURE REVIEW

2.1 SODIUM ION BATTERY

A sodium-ion battery (sometimes NIB) is a member of a family of rechargeable battery types in which sodium ions move from the negative electrode to the positive electrode during discharge, and back when charging. This type of battery is still under development and unlike sodium batteries sodium ion batteries can be made portable and are able to work at room temperature (approx. 25˚C).

2.2 NIB COMPONENTS

The components are as [6]: negative electrode, positive electrode and Electrolyte.

Positive electrode materials for sodium ion batteries are as[7]: a layered oxide (such as Sodium cobalt oxide), a polyanion (such as Sodium iron phosphate), a spinel (such as sodium manganese oxide), an olivine.

Negative electrode materials for sodium ion batteries: Carbon Materials, Low Potential Metal Phosphates, Low Potential Sodium Metal Oxides, Alloys

The electrolyte is typically a mixture of organic carbonates such as ethylene carbonate or diethyl carbonate containing complexes of sodium ions. These non-aqueous electrolytes generally use non-coordinating anion salts such as sodium hexafluorophosphate ($NaPF_6$), sodium hexafluoroarsenate monohydrate ($NaAsF_6$), sodium perchlorate ($NaClO_4$), sodium tetrafluoroborate ($NaBF_4$), and sodium triflate ($NaCF_3SO_3$).

2.3 REACTIONS INVOLVED

- At Cathode
- $NaCoO_2 \longleftrightarrow Na_{1-x}CoO_2 + xNa^+ + xe^+$

- At Anode
- $C_n + xNa^+ + xe^+ \longleftrightarrow C_nNa_x$
- Overall
- $NaCoO_2 + C_n \longleftrightarrow Na_{1-x}CoO_2 + C_nNa_x$

Pure sodium is very reactive. It reacts vigorously with water to form sodium hydroxide and hydrogen gas. Thus, a non-aqueous electrolyte is typically used, and a sealed container rigidly excludes water from the battery pack.

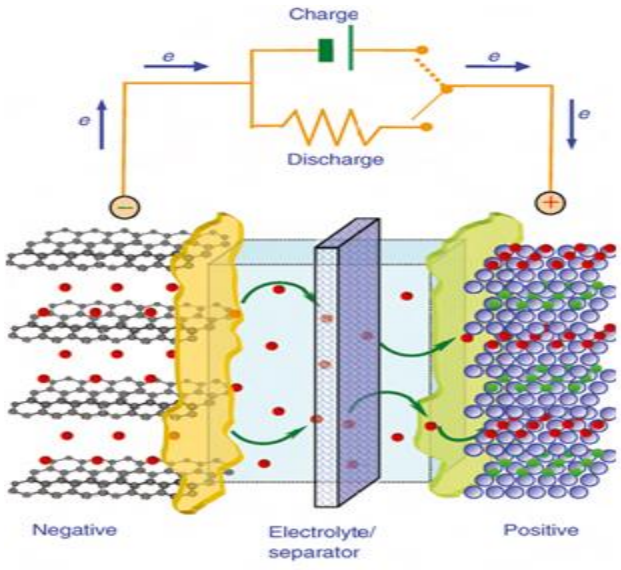

Figure 3: SCHEMATIC ILLUSTRATION OF A RECHARGEABLE SODIUM BATTERY

2.4 CHARGE AND DISCHARGE

During charging an external power source(the charging circuit) applies an over voltage(a higher voltage but of same polarity) than that by the battery, forcing the current to pass in the reverse direction[8]. The sodium ions then migrate from the positive to negative electrode, where they become embedded in the porous electrode material in the process

known as intercalation. During discharge, sodium ions carry current from the negative to the positive electrode, through the non-aqueous electrolyte and the separator diaphragm[8].

2.5 **LAYEREDCOMPOUNDSAS CATHODE MATERIAL**

Among all the sodium based cathode material reported till now, layered transition-metal oxides (Na_xMO_2, M = transition-metal) have attracted attention, because of their potential high capacity, provide spacious diffusion path, structural stability and their open structures can accommodate large sodium-ions. The layered Na_xMO_2 materials can be classified into two main groups:

1. P2 type: the first letter 'P' refers to the prismatic site occupied by the alkali ion. The digit '2' refers to the number of transition metal layers in the repeat unit perpendicular to the layering.
2. O3 type: the first letter 'O' refers to the octahedral site occupied by the alkali ion[9].

The deintercalation and intercalation of sodium in various layered Na_xMO_2 has been reported for a very wide variety of transition metals as briefly outlined in a recent report[10]. These oxides consists of Na_xCoO_2[11,12], Na_xMnO_2[13,14],Na_xaCrO_2[15],Na_xVO_2[16], and their binary and ternary derivatives, which candeliver capacity greater than or equal to 120 mA h g^{-1}. Out of these , the manganese and cobalt oxides are the most viable for positive electrodes. However, these materials usually undergo multiple phase transitions during sodium insertion/extraction reactions, showing several voltage steps in their charge/discharge profiles. Possibly because of the complicated and multiple phase transformations, these layered oxides suffer from cycling instability with continuous capacity decay upon cycling. Another drawback of these materials is that some of them could not tolerate deep charging at a potential over 4.0 V (vs. Na+/Na), resulting to an incomplete utilization of their sodium ion storage capacity. Once charged to 4.2 V or more, these materials degrade considerably with large irreversible capacity loss, due to sodium-driven structural, irreversible changes.

Also the Jahn-Teller distortion of Mn(III) is the most prominent factor which decides the structural stability for Mn-based oxides during ion insertion.To overcome these problems, a

general strategy applied to sodium based layered oxides is to substitute partial metal ions in the transition metal layer using selected cations, so as to improve the structural stability and electrochemical performances of the Layered hosts. In recent years, many attempts have been devoted to synthesize the solid solutions of layered $Na_xMn_{1-y}M_yO_2$ (M = Ni,Co, Fe, etc.) with the aim to obtain low cost and high capacity sodium insertion cathodes. Hence various attempts have been made to synthesize the ternary derivatives of Na_xMnO_2. Some of them are:

(1) $Na_{0.67}Mn_{0.65}Co_{0.2}Ni_{0.15}O_2$

(2) $Na_{0.45}Mn_{0.66}Co_{0.11}Ni_{0.22}O_2$

(3) $Na_{.67}Mn_{.65}Fe_{0.20}Ni_{0.15}O_2$

The drawbacks of $Na_{0.67}Mn_{0.65}Co_{0.2}Ni_{0.15}O_2$ and $Na_{0.45}Mn_{0.66}Co_{0.11}Ni_{0.22}O_2$ is that the cobalt is toxic and expensive. So combining the strategies of transition metal intermixing with the implementation of smaller cations inside the material is a promising method to improve the stability of layered sodium-based cathode materials. More the Ni-substitution could provide smoother phase transformation so as to improve the cycling stability. Therefore, the Ni-substitution Mn-Fe-based oxide is a promising cathode material with high capacity and good cycling stability for high-performance sodium ion batteries.

Hence the structure, morphology and the composition of $Na_{0.67}Mn_{0.65}Fe_{0.20}Ni_{0.15}O_2$wasstudied using X-ray Diffraction, Scanning Electron Microscopy and energy dispersive X-ray spectroscopy (EDX) respectively.

CHAPTER 3:SYNTHESIS AND CHARACTERIZATION OF $Na_{0.67}Mn_{0.65}Fe_{0.20}Ni_{0.15}O_2$

3.1 SYNTHESIS

NaMFN sample was prepared by using citric acid assistedsol-gel synthesis. Stoichiometric amount of Sodium Acetate, Manganese Acetate, Iron Nitrate and Nickel Acetate were separately mixed in de-ionized water unless they were completely dissolved. Then the mixed solution was added drop wise into a citric acid solution(weighing 1.5times the mass of $CH_3COONa.3H_2O$, $(CH_3COO)_2Mn.4H_2O$, $Fe(NO)_3.9H_2O$ & $Ni(CH_3COO)_2.4H_2O$ collectively).The resulting solution was heated at 80^0C and stirred for six hours at 370rpm as shown in figure 4. Ammonia was added to the green sol mixture to adjust the pH. A clear and viscous gel of green colour was obtained.

Figure 4: MAGNETIC STIRRER

.

The resulting gel was dried at 110^0C for twenty four hours in hot air oven as shown in Figure 5.

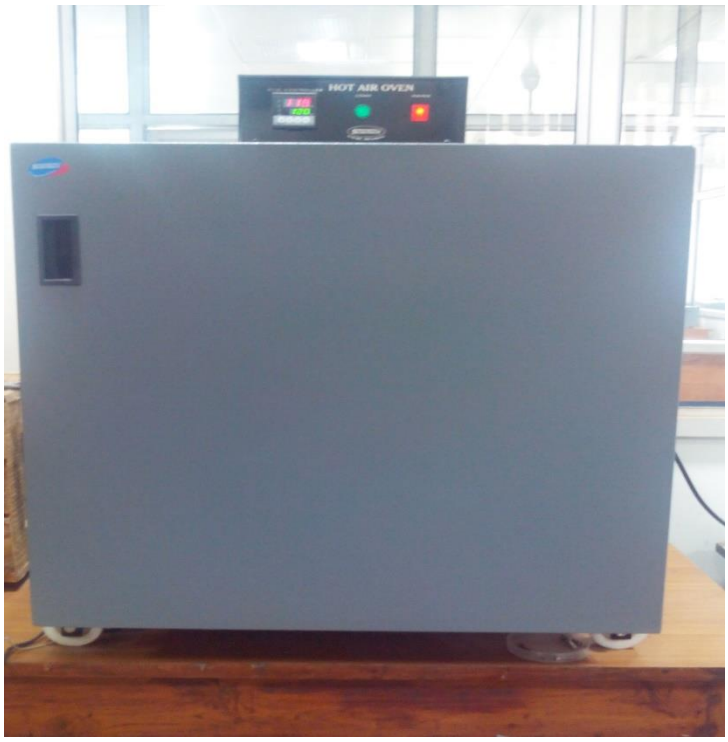

Figure 5: HOT AIR OVEN

The resulting precursor was grinded in mortar and pestle and then decomposed at 300^0C in air for six hours in tubular furnace. The solid precursor was then again ground in mortar and pestle as shown in Figure 6.

Figure 6: MORTAR AND PESTLE

Then it was left for cooling, which was again grinded and then calcined at 800^0C for fifteen hours at 5^0C.min^{-1} in air as shown in Figure 7. Finally it was again grinded to obtain the final product.

Mixing of stoichiometric ratios of $CH_3COO\ Na.3H_2O$, $(CH_3COO)_2Mn.4H_2O$, $Fe(NO)_3.9H_2O$ & $Ni(CH_3COO)_2.4H_2O$ with citric acid

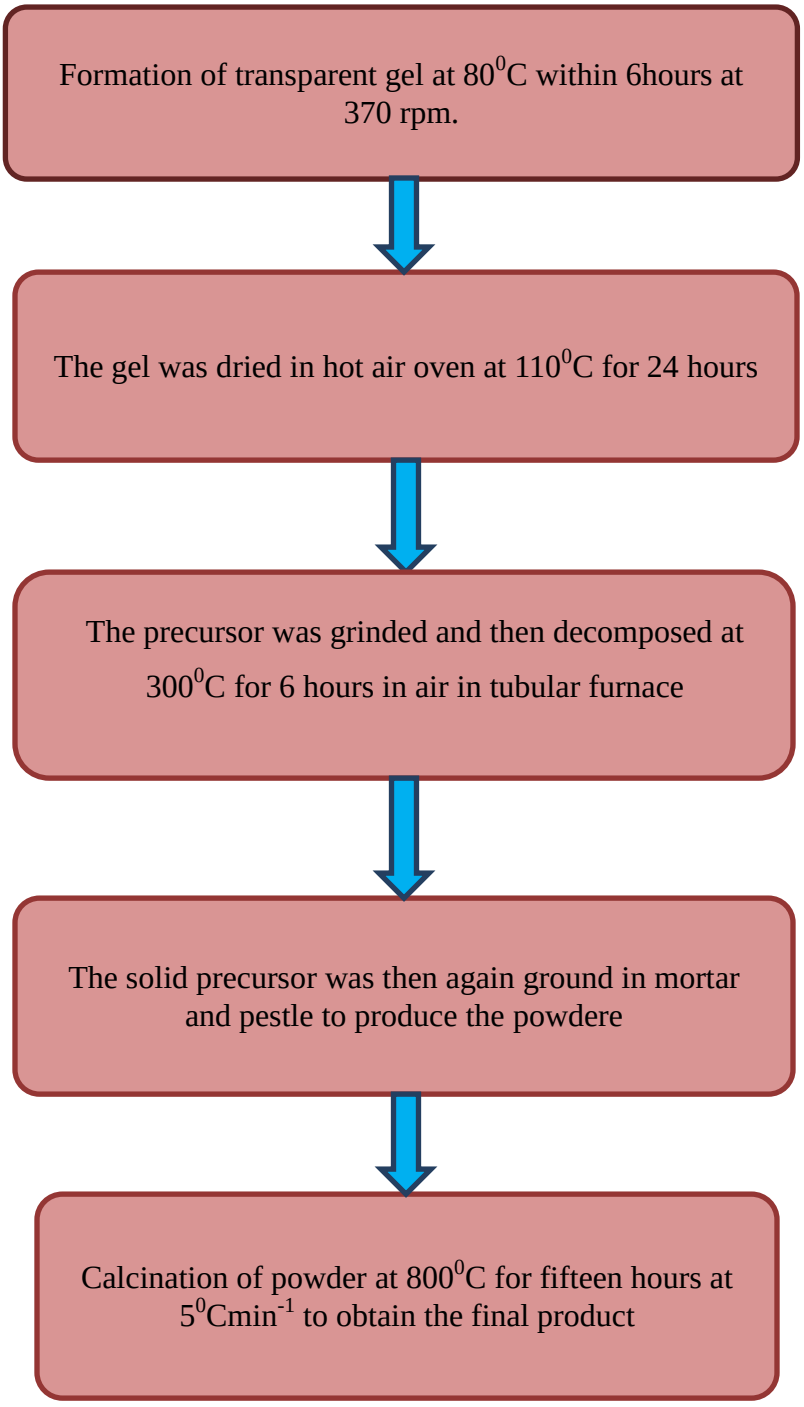

Figure 8: FLOWCHART OF SYNTHESIS PROCESS OF

$Na_{0.67}Mn_{0.65}Fe_{0.20}Ni_{0.15}O_2$

3.2CHARACTERIZATIONTECHNIQUES

XRD and SEM have been done in order to characterize the synthesized $Na_{0.67}Mn_{0.65}Fe_{0.20}Ni_{0.15}O_2$ and to study the structure and morphology of the material.

3.2.1 X-RAY DIFFRACTION CHARACTERIZATION

X-ray powder diffraction (XRD) is an analytical technique basicaly used for phase identification of a crystalline material and even can provide information on unit cell dimensions. The principle of XRD is Max von Laue, in 1912, discovered that crystalline substances act as three-dimensional diffraction gratings for X-ray wavelengths similar to the spacing of planes in a crystal lattice. X-ray diffraction is now a common technique for the study of crystal structures and atomic spacing[18].

X-ray diffraction is based on constructive interference of monochromatic X-rays and a crystalline sample. These X-rays are generated by a cathode ray tube, filtered to produce monochromatic radiation, collimated to concentrate, and directed toward the sample. The interaction of the incident rays with the sample produces constructive interference (and a diffracted ray) when conditions satisfy Bragg's Law ($n\lambda=2d \sin\theta$). This law relates the wavelength of electromagnetic radiation to the diffraction angle and the lattice spacing in a crystalline sample. These diffracted X-rays are then detected, processed and counted. By scanning the sample through a range of 2θangles, all possible diffraction directions of the lattice should be attained due to the random orientation of the powdered material. Conversion of these diffraction peaks to d-spacings allows the identification of the mineral because each mineral has a unique set of d-spacings. This is achieved by comparison of d-spacings with standard reference patterns. The basic elements of X-ray diffractometers are as: an X-ray tube, a sample holder, and an X-ray detector.

Figure 9: BRUKER'S X-RAY DIFFRACTION INSTRUMENT

X-rays are generated in a cathode ray tube by heating a filament to produce electrons, accelerating the electrons toward a target by applying a voltage, and bombarding the target material with electrons. When electrons have sufficient energy to dislodge inner shell electrons of the target material, characteristic X-ray spectra are produced. These spectra consist of several components, the most common being K_α and K_β. K_α consists, in part, of $K_{\alpha 1}$ and $K_{\alpha 2}$. $K_{\alpha 1}$ has a slightly shorter wavelength and twice the intensity as $K_{\alpha 2}$. The specific wavelengths are characteristic of the target material (Cu, Fe, Mo, Cr). Filtering, by foils or crystal monochrometers, is required to produce monochromatic X-rays needed for diffraction. $K_{\alpha 1}$and $K_{\alpha 2}$are sufficiently close in wavelength such that a weighted average of the two is used. Copper is the most common target material for single-crystal diffraction, with CuK_α radiation = 1.5418Å. These X-rays are collimated and directed onto the sample. As the sample and detector are rotated, the intensity of the reflected X-rays is recorded. When the geometry of the incident X-rays impinging the sample satisfies the Bragg Equation, constructive interference occurs and a peak in intensity occurs. A detector records and processes this X-ray signal and converts the

signal to a count rate which is then output to a device such as a printer or computer monitor.

The geometry of an X-ray diffractometer is such that the sample rotates in the path of the collimated X-ray beam at an angle θ while the X-ray detector is mounted on an arm to collect the diffracted X-rays and rotates at an angle of 2θ. The instrument used to maintain the angle and rotate the sample is termed a goniometer. For typical powder patterns, data is collected at 2θ from ~5° to 70°, angles that are preset in the X-ray scan.

3.2.2 SCANNING ELECTRON MICROSCOPE

Figure 10: HITACHI S-3700N SEM SYSTEM

The scanning electron microscope (SEM) uses a focused beam of high-energy electrons to generate a variety of signals at the surface of solid specimens. The signals that derive from electron-sample interactions reveal information about the sample including external morphology (texture), chemical composition, and crystalline structure and orientation of materials making up the sample. In most applications, data are collected over a selected area of the surface of the sample, and a 2-dimensional image is

generated that displays spatial variations in these properties. Areas ranging from approximately 1 cm to 5 microns in width can be imaged in a scanning mode using conventional SEM techniques (magnification ranging from 20X to approximately 30,000X, spatial resolution of 50 to 100 nm). The SEM is also capable of performing analyses of selected point locations on the sample; this approach is especially useful in qualitatively or semi-quantitatively determining chemical compositions (using EDS), crystalline structure, and crystal orientations (using EBSD). The design and function of the SEM is very similar to the EPMA and considerable overlap in capabilities exists between the two instruments[15]. The principle of SEM is:

Accelerated electrons in an SEM carry significant amounts of kinetic energy, and this energy is dissipated as a variety of signals produced by electron-sample interactions when the incident electrons are decelerated in the solid sample. These signals include secondary electrons (that produce SEM images), backscattered electrons (BSE), diffracted backscattered electrons (EBSD that are used to determine crystal structures and orientations of minerals), photons (characteristic X-rays that are used for elemental analysis and continuum X-rays), visible light (cathodoluminescence–CL), and heat. Secondary electrons and backscattered electrons are commonly used for imaging samples: secondary electrons are most valuable for showing morphology and topography on samples and backscattered electrons are most valuable for illustrating contrasts in composition in multiphase samples (i.e. for rapid phase discrimination). X-ray generation is produced by inelastic collisions of the incident electrons with electrons in discrete orbitals (shells) of atoms in the sample. As the excited electrons return to lower energy states, they yield X-rays that are of a fixed wavelength (that is related to the difference in energy levels of electrons in different shells for a given element). Thus, characteristic X-rays are produced for each element in a mineral that is "excited" by the electron beam. SEM analysis is considered to be "non-destructive"; that is, x-rays generated by electron interactions do not lead to volume loss of the sample, so it is possible to analyze the same materials repeatedly.

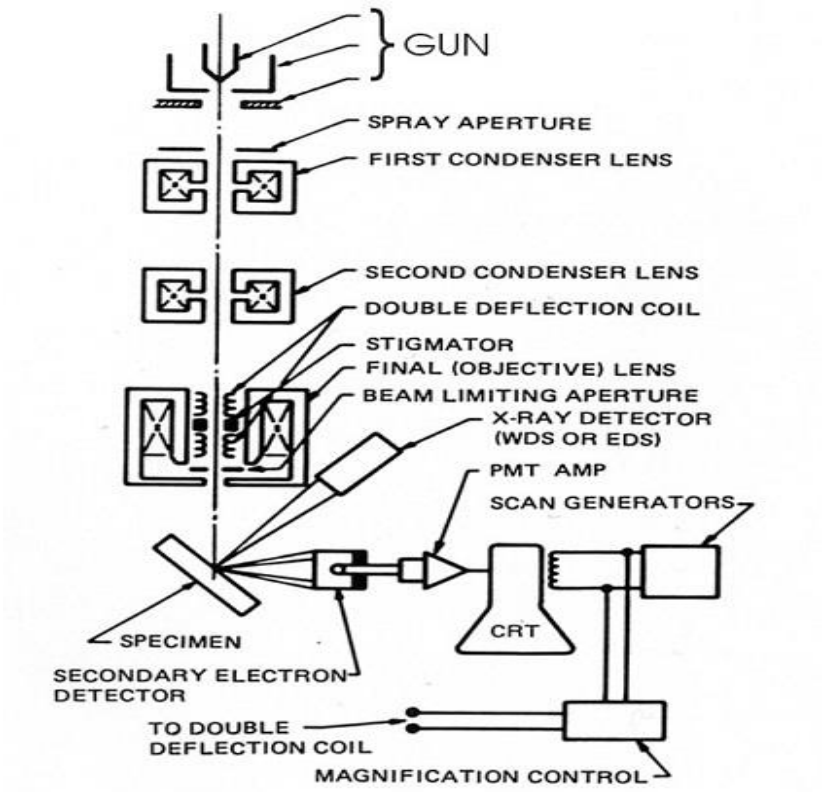

Figure 11: SCHEMATIC SHOWING THE WORKING OF SEM

CHAPTER 4: RESULTS AND DISCUSSION

X-ray diffraction (XRD) of calcined sample$Na_{0.67}Mn_{0.65}Fe_{0.20}Ni_{0.15}O_2$ at 800^0C for twelve hours in air has been carried out and shown in figure 12. XRD was used to identify the chemical phase(s) and presence of any crystalline impurities in the sample material. The structure of the cathode material $Na_{0.67}Mn_{0.65}Fe_{0.20}Ni_{0.15}O_2$ has been evaluated with an X-ray diffractometer using filter Cu $K\alpha_1$ radiation by measuring the diffraction angle (2θ) between $10^0$and 80^0 with ascanning rate of $2^0min^{-1}$and a step size of 0.02^0.

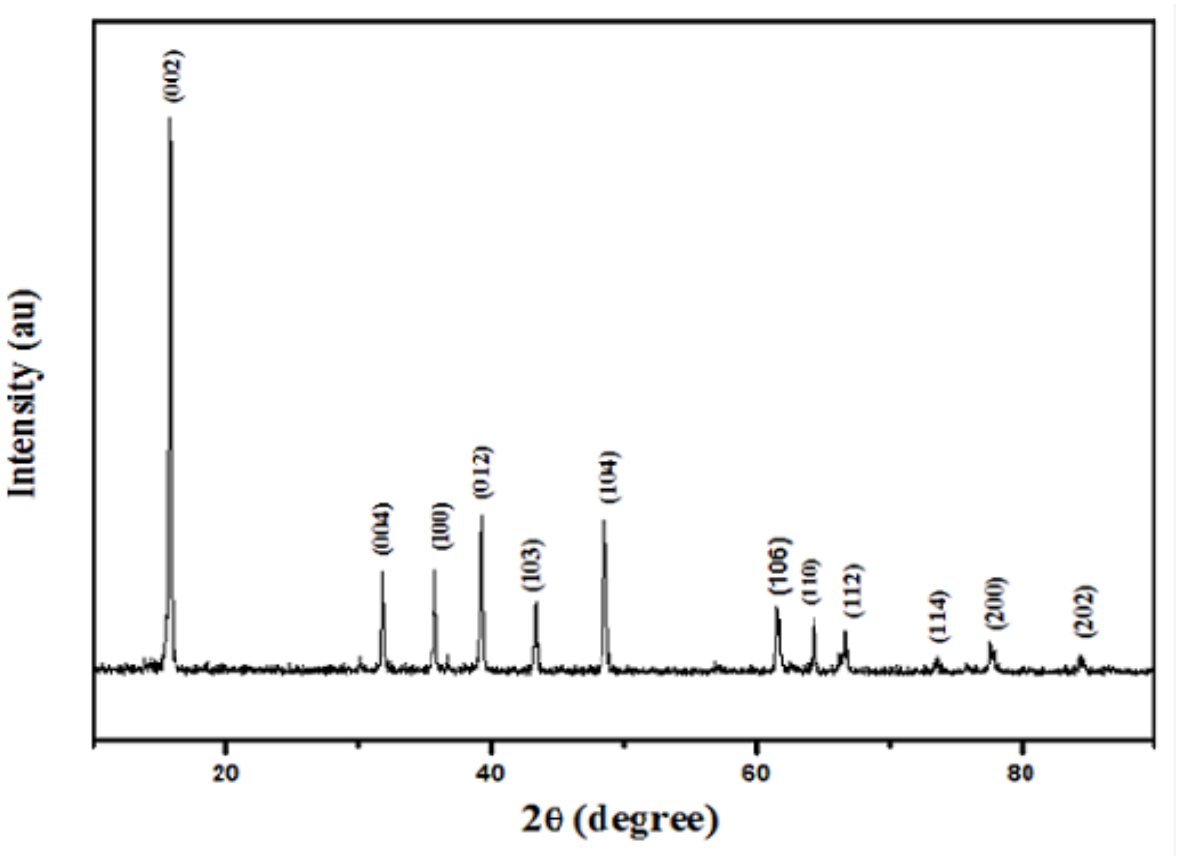

Figure 12: XRD PATTERN OF$Na_{0.67}Mn_{0.65}Fe_{0.20}Ni_{0.15}O_2$CALCINED AT 800^0C FOR TWELVE HOURS IN AIR

From the above XRD pattern we conclude that

S.No.	Peak obs. [°2Th]	Miller Indices
1.	15.639	002
2.	31.932	004
3.	35.749	100
4.	39.311	012
5.	43.242	103
6.	48.671	104
7.	61.705	106
8.	66.420	110
9.	66.625	112
10.	73.524	114

The strongest peak of the sample. The 2-theta of the peak with miller indices (002) is 15.639^0. The FWHM of this peak is 0.1763747^0.The sample shows almost the same XRD features and all the diffraction lines appear similarly to their parent P2-$Na_{2/3}MnO_2$[19],$Na_{2/3}[Mn_{1-x}Ni_x]O_2$[19], $Na_{0.67}Mn_{0.65}Co_{0.2}Ni_{0.15}O_2$ [20] and$Na_{0.45}Mn_{0.66}Co_{0.11}Ni_{0.22}O_2$[21] compounds.No impurity peaks were found in the diffraction pattern, suggesting that all the substituted metal enters the transition-metal layers.

The crystallographic parameters of $Na_{0.67}Mn_{0.65}Fe_{0.20}Ni_{0.15}O_2$ according to literature are as follows: the Crystal Structure is hexagonal structure and the Space group is$P6_3/mmc$[20].The crystallite size of $Na_{0.67}Mn_{0.65}Fe_{0.20}Ni_{0.15}O_2$ corresponding to the highest peak is 45.4511618nm.

Figure 13[20] shows the diagrammatic presentation of the P2-type structure of the Na_xMO_2 phases[22].The Na ions in prismatic sites are sandwiched between the MO_2sheets to form layered structure. It is observed clearly that the repetitive unit number of MO_2sheets is 2 and the sodium-ions in prismatic site have two different types: Na_f and Na_e which shares face or edge with MO_6octahedra, respectively. The two sites are simultaneously occupied by sodium-ions to minimize electrostatic repulsion between sodium ions.

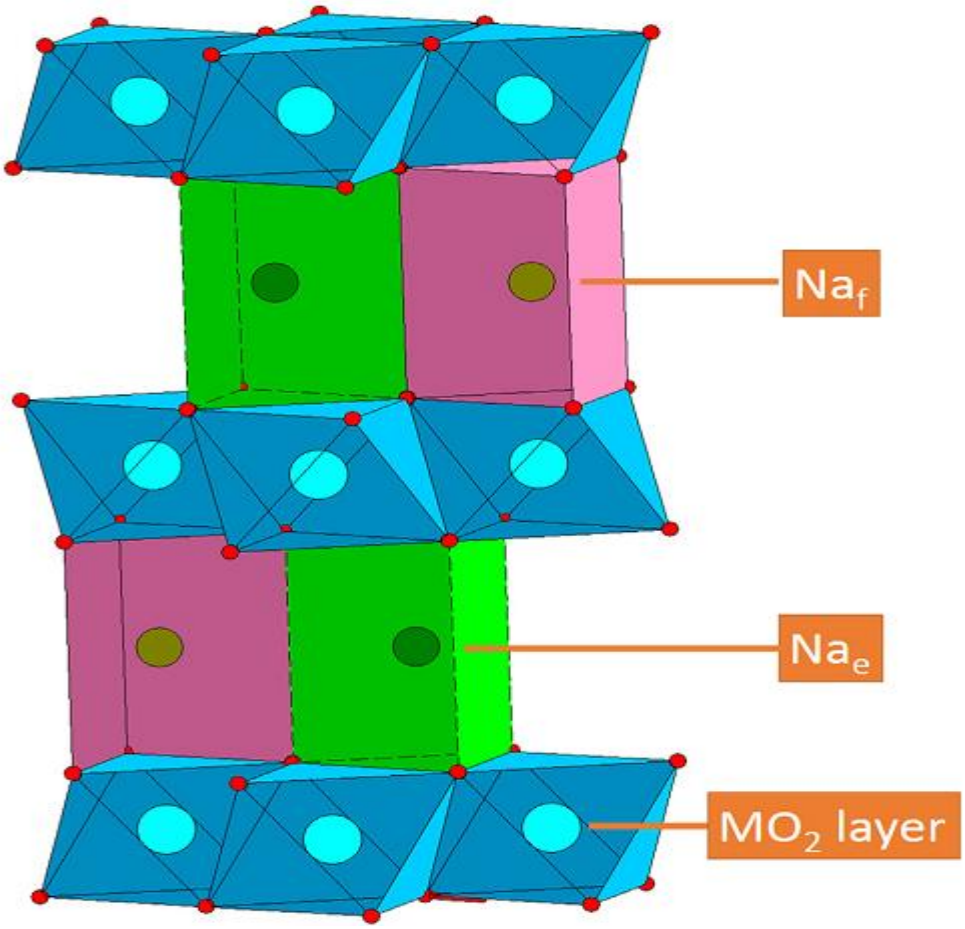

Figure 13: DIAGRAMMATIC PRESENTATION OF THE P2-TYPE STRUCTURES OF THE Na_xMO_2 PHASES.

Scanning Electron Microscopy was carried out utilizing a HITACHI S-3700N SEM system. The SEM images of the NaMFN material used in this study is as shown in figure 14:

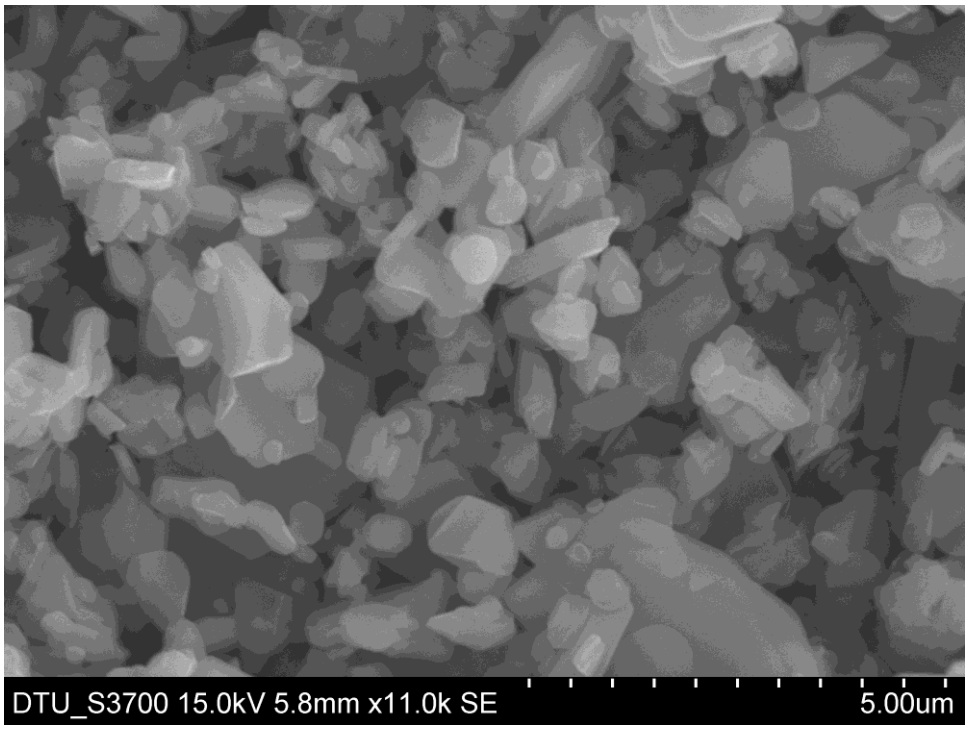

Figure 14(a): SEM IMAGE OF $Na_{0.67}Mn_{0.65}Fe_{0.20}Ni_{0.15}O_2$5µm CALCINED AT 800^0C FOR TWELVE HOURS IN AIR

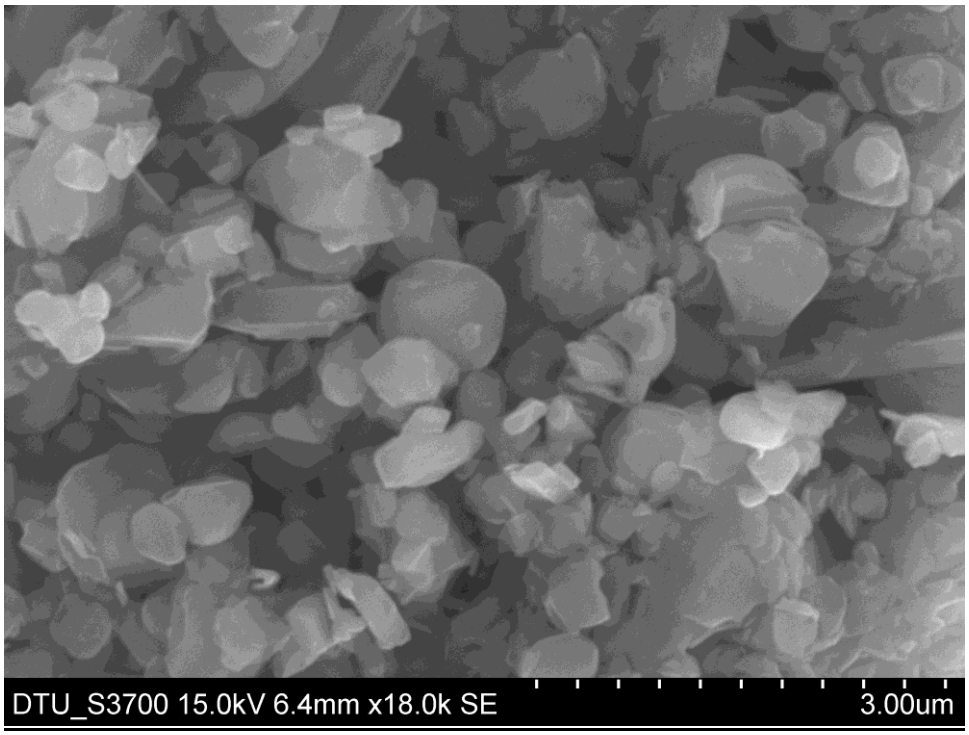

Figure 14(b) SEM IMAGE OF $Na_{0.67}Mn_{0.65}Fe_{0.20}Ni_{0.15}O_2$3µm CALCINED AT 800^{0}C FOR TWELVE HOURS IN AIR

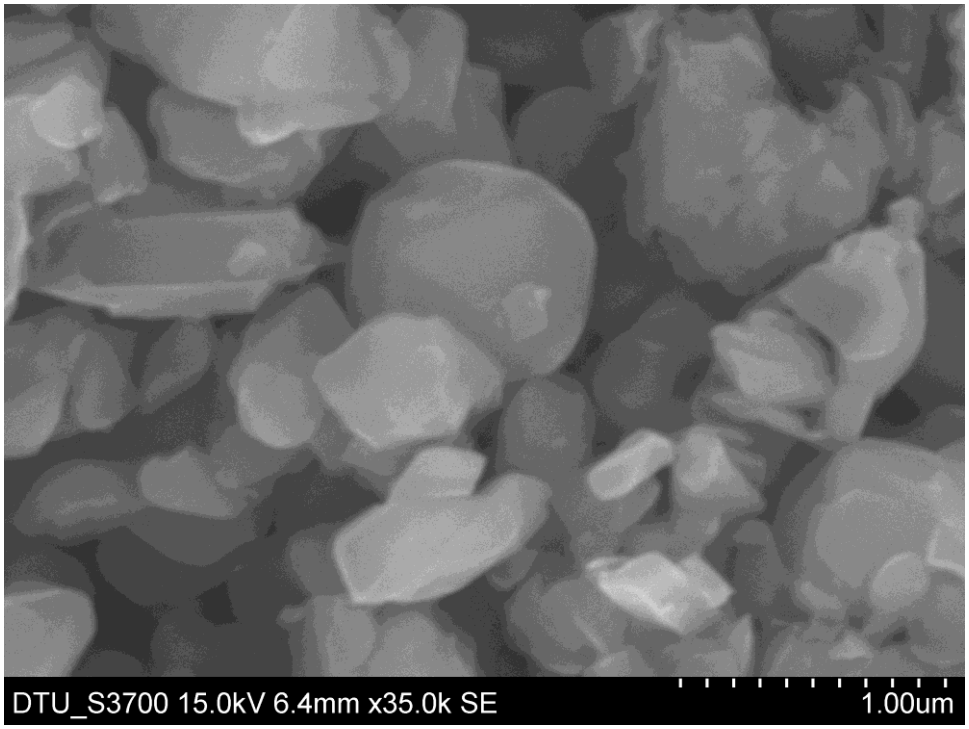

Figure 14(c) : SEM IMAGE OF $Na_{0.67}Mn_{0.65}Fe_{0.20}Ni_{0.15}O_2$1µm CALCINED AT 800^{0}C FOR TWELVE HOURS IN AIR

From the above SEM images it is found that most of the particles with mixed shape of plate and spherical nature with uneven distribution are formed. The average size of particles lies in the range of 200nm-600nm.

CHAPTER 5: CONCLUSION

Following conclusion can be drawn from the present study: A sodium based$Na_{0.67}Mn_{0.65}Fe_{0.2}Ni_{0.15}O_2$ layered material was synthesized by sol-gel method with citric acid as chelating agent. There were no impurity peaks found in the diffraction pattern of the layered material, suggesting that all the substituted metal enters the transition-metal layer.SEM images show most of the particles exhibit plate-shaped particles, though the distribution of the particles is uneven.XRD confirms the hexagonal P2-structure with the space group $P6_3/mmc$ (Ref No. 194) is formed.

REFERENCES

[1] Bo Xu, Danna Qian, Ziying Wang, Ying Shirley Meng, Recent progress in cathode materials research for advanced lithium ion batteries, Materials Science and Engineering,73, **2012**, 51–65.

[2] JiajunChen, Recent Progress in Advanced Materials for Lithium Ion Batteries, Materials, 6, **2013**, 156-183.

[3] MajaPivko, IztokArcon, MarjanBele, Robert Dominkoa, MiranGaberscek, $A_3V_2(PO_4)_3$ (A= Na or Li) probed by in situ X-ray absorption spectroscopy“ , Journal of Power Sources, 216, **2012**, 145-151.

[4] Brian L. Ellis, Linda F. Nazar, Sodium Opinion in Solid State and Materials Science, Current Opinion in Solid State and Materials Science, 16, **2012**, 168-177.

[5] Kuniko Chihara, AyukoKitajou, Irina D. Gocheva, Shigeto Okada, and Jun-ichiYamaki, Cathode Properties of $Na_3M_2(PO_4)_2F_3$ [M=Ti, Fe, V] for Sodium-Ion Batteries, Journal of Power Sources, 227, **2013**, 80-85.

[6] Andrew Ritchie, Wilmont Howard, Recent developments and likely advances in lithium-ion batteries, Journal of Power Sources, 162, **2006**, 809-812.

[7] Brian L. Ellis, Linda F. Nazar, Sodium and sodium-ion energy storage batteries, Current Opinion in Solid State and Materials Science, 16, **2012**, 168-177.

[8] O.Toprakci, H. Toprakci, L. Ji, X. Zhang, Fabrication and Electrochemical Characteristicsof LiFePO4 Powders for Lithium–Ion Batteries, Kona Powder and Particle Journal, 28, **2010**, 50-72.

[9] C. Delmas et al, Physica B & C 99, **1980**, 81.

[10] Ma X, Chen H, Ceder G. Electrochemical properties of monoclinic $NaMnO_2$, J ElectrochemSoc, 158, **2011**, A1307.

[11] A. Bhide and K. Hariharan, Solid State Ionics, 192,**2011**, 360**–**363.

[12] I. Saadoune, A. Maazaz, M. Menetrier and C. Delmas, J. Solid State Chem., 122, **1996**, 111–117.

[13] A. Caballero, L. Hernan, J. Morales, L. Sanchez, J. Santos Pena and M. A. G. Aranda, J. Mater. Chem., 12, **2002**, 1142–1147.

[14] X. Ma, H. Chen and G. Ceder, J. Electrochem. Soc., 158, **2011**, 1307–1312.

[15] S. Komaba, C. Takei, T. Nakayama, A. Ogata and N. Yabuuchi, Electrochem. Commun., 12, **2010**, 355–358.

[16] D. Hamani, M. Ati, J.-M. Tarascon and P. Rozier, Electrochem. Commun., 13, **2011**, 938–941.

[17] Bettina Voutou, Eleni-ChrysanthiStefanaki, Electron Microscopy: The Basics, Physics of Advanced Materials Winter School 2008.

[18] B.D. Cullity, Elements Of X-Ray Diffraction, 85, 1956.

[19] J. M. Paulsen and J. R. Dahn, Solid State Ionics, 126, **1999**, 3–24

[20]Dingding Yuan, Wei He, Feng Pei, Fayuan Wu, Yue Wu, JiangfengQian, Yuliang Cao, XinpingAib and Hanxi Yang, Synthesis and electrochemical behaviors of layered $Na_{0.67}Mn_{0.65}Co_{0.2}Ni_{0.15}O_2$ microflakes as a stable cathode material for sodium-ion batteries, J. Mater. Chem. A, 1, **2013**, 3895-3900.

[21] Daniel Buchholz, Luciana Gomes Chagas, Martin Winter1, Stefano Passerini, P2-type layered $Na_{0.45}Mn_{0.66}Co_{0.11}Ni_{0.22}O_2$as intercalation host material for lithium and sodium batteries, ElectrochimicaActa, 110, **2013**, 208–213.

[22] Jing Xu, Dae Hoe Lee and Ying Shirley Meng, Recent advances in sodium intercalation positive electrode materials for sodium ion batteries, 6, **2013**, 1330001-1330007